Materials Physics and Mechanics 42 (2019) 389-395 Received: March 26, 2019

DYNAMIC FRACTURE OF CERAMIC PLATES DUE TO IMPACT LOADING. NUMERICAL INVESTIGATION

V.A. Bratov, N.A. Kazarinov*

Saint Petersburg State University, Saint Petersburg, Universitetskaya emb., 7-9, Russia

Institute of problems of mechanical engineering, Saint Petersburg, Bolshoi av. 61, Russia

*e-mail: n.kazarinov@spbu.ru

Abstract. The paper presents comparative numerical analysis of two ceramic materials subjected to impact loading. ZrO2(Y2O3) and Al2O3 ceramics are studied. The main objective of the work is to study influence of various material parameters on ballistic performance of ceramic materials and on characteristics of the dynamic fragmentation process. The applied numerical scheme is based on finite element method and incubation time fracture criterion. Results on fracture surface area, residual impactor velocity, fragment size distribution are reported for the two materials and various impactor velocities.
Keywords: impact, ceramics, dynamic fracture, fragmentation, FEM

1. Introduction

Investigation of dynamic fracture of ceramic materials is of high importance for engineering applications. These brittle materials are successfully used in protection systems (armor, bulletproof vests) due to their remarkable mechanical properties. From one hand ceramics exhibit high strength (when manufactured appropriately), on the other hand ceramic materials are able to absorb considerable amount of impact energy due to extensive fragmentation and thus can be used as a sacrificial material in the protective systems [1].

In order to efficiently design ceramic protection systems which are supposed to operate in the impact loading conditions, one should be able to predict dynamic fracture of the ceramic materials. Since analytical solutions for the real-life problems (finite sample dimensions, arbitrary paths of the crack propagation, etc.) are not available, numerical simulation appears to be the only possible way to optimize the material choice for a certain engineering application. Numerical schemes applied for the impact simulation should account for dynamic peculiarities of the fracture process and thus appropriate fracture conditions should to be used.

The numerical scheme which uses incubation time fracture criterion [2] has been applied in this work. This fracture model has been successfully used to predict initiation and development of the dynamic fracture for a wide range of brittle and quasi-brittle materials subjected to dynamic loading [3]. The developed scheme is based on finite element method in a two-dimensional axisymmetric formulation. Such problem statement implies restrictions on sample and impactor geometry requiring them to be axially symmetric. Additionally, no radial cracks can be simulated using the two-dimensional scheme. However, such approach is computationally efficient and provides possibility to compare (at least qualitatively) materials with different mechanical properties and therefore choose the most suitable material for certain loading conditions.

http://dx.doi.org/10.18720/MPM.4242019_3

Impact fracture of equally shaped Al2O3 and ZrO2(Y2O3) round specimens was studied. In both cases cylindrical steel impactor was used. Dependence of the fracture surface area on the impactor velocity was calculated for the two materials. In addition to this dynamic fragmentation of the ceramic targets was numerically investigated.

2. Incubation time fracture model

The incubation time fracture criterion was proposed in [2,4]. According to this fracture criterion if the following inequality holds, fracture at point x and time t takes place:

$$\frac{1}{\tau}\int_{t-\tau}^{t}\frac{1}{d}\int_{x-d}^{x}\sigma(x',t')dx'dt' \geq \sigma_c. \quad (1)$$

In the criterion (1) $\sigma(x,t)$ is a time-dependent stress and σ_c is the ultimate stress for the studied material. Criterion (1) contains linear size d, which can have various interpretations, however the incubation time approach implies d to be the fracture process zone size, indicating minimal increment of the fracture surface growth. The parameter d can be calculated according to the formula $d = 2K_{IC}^2/\pi\sigma_C^2$, where K_{IC} is the critical stress intensity factor of the studied material. The criterion (1) is able to account for preparatory microscopic processes (e.g. microcracking, evolution of voids and defects, etc.) leading to the macroscopic fracture. These processes require time to evolve, and this time is considered to be a material property – the incubation time. This way, macroscopic fracture is regarded as a non-instantaneous event and various effects of the dynamic fracture can be studied and predicted using (1).

The incubation time criterion has been successfully used for a wide variety of problems [3] including dynamic crack propagation in different loading regimes, solid particle erosion studies [5].

3. Simulation methods

The incubation time approach provides possibility to account for essentially non-linear fracture processes while solving the linearly stated problem. Both materials (ceramic target and steel impactor) are considered to be elastic and corresponding material properties are listed in Table 1 [6,7,8]. The target has the following dimensions: 100 mm in diameter and 10 mm thick, while the steel impactor is 100 mm long and its diameter is 10 mm. The developed numerical scheme is based on finite element method in a two-dimensional axisymmetric formulation. ANSYS solver is used to calculate the stress-strain state of the target and custom routines were developed in order to implement criterion (1) and to control the solution flow. Figure 1 shows a part of the finite element mesh and a full model with symmetry expansion applied.

Table 1. Material properties (dash indicates that the parameter was not used in the computations

	Al2O3	ZrO2(Y2O3)	Steel projectile
Young's modulus, E, GPa	366	200	200
Poisson's ratio, ν	0.21	0.25	0.25
Density, ρ, kg/m^3	3880	6000	7860
Ultimate stress, σ_c, MPa	260	750	–
Incubation time, τ, μs	1	1	–

The mesh for the finite element solution was constructed manually in the presented case. Elements do not share nodes, however nodes with equal coordinates have coupled degrees of freedom acting as a single node. This restriction is maintained until condition (1) holds. When fracture occurs according to (1), nodes are decoupled and elements are separated

leading to the fracture surface generation (see Fig. 2). Since axial symmetry is applied, each crack contributes to the total fracture surface area (S) according to equation $S = S + 4d * 2\pi R$, where R is distance between the crack and the symmetry axis.

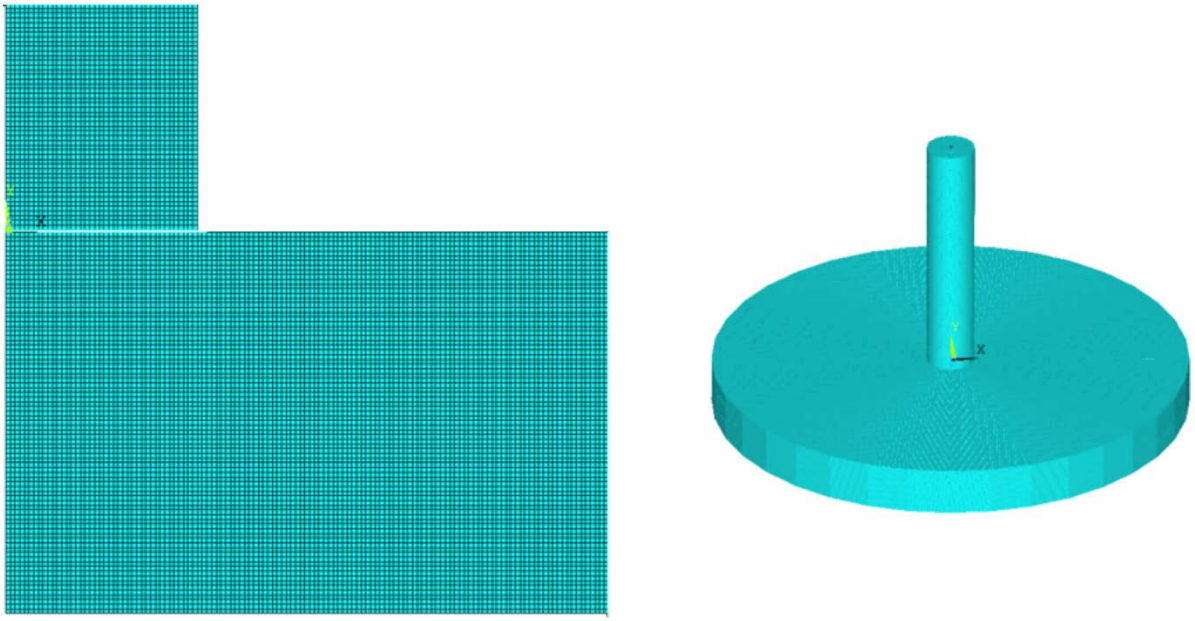

Fig. 1. Part of them finite element mesh (contact zone) and full model with symmetry expansion applied

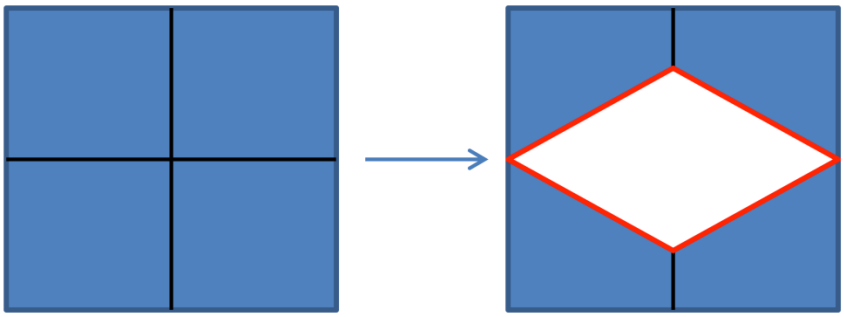

Fig. 2. Decoupling of the matching nodes and fracture surface generation

Element size equals d and thus minimal fracture increment is also d which lies within the incubation time approach framework. The solution time step is chosen to be smaller than the time needed for the fastest wave to travel the d distance.

In order to investigate fragmentation of the ceramic targets a separate program was developed. The finite element mesh is regarded as a graph with the mesh elements being nodes of the graph. This way, separate fragments of the target are connected components of the element graph.

4. Results

Fracture surface area. This section presents results of the fracture surface area calculations. Figure 3 shows typical evolution of the fracture surface are on time: abrupt growth of the surface area indicates active cracking of the sample and the fracture surface area value reaches its maximum and stops growing when the fracture process is completed.

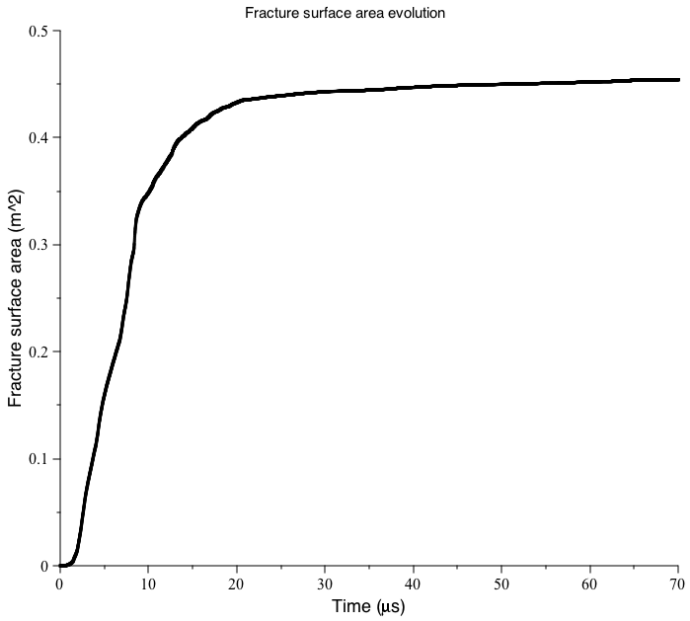

Fig. 3. Fracture surface area evolution. The data for the Al2O3 target and 350 m/s impactor velocity is presented

The computations were made with 1 μs incubation time parameter for the both materials. The dependence of the fracture surface area on the impactor velocity is shown in Fig. 4. For the studied regimes the fracture surface area increases with the growing impactor velocity for the Al2O3 material. However, the results stabilize for the ZrO2(Y2O3) ceramics. This might indicate that maximal level of energy absorption has been reached by the dynamic fracture process.

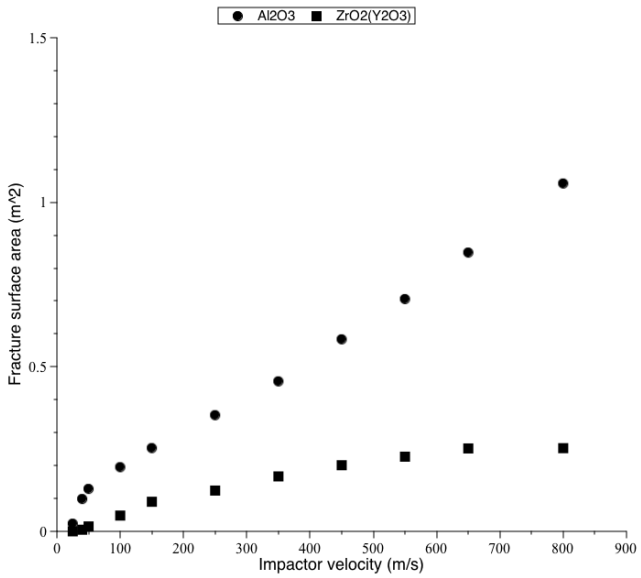

Fig. 4. Fracture surface area versus impactor velocity dependence

Residual impactor velocity. Here dependence of the residual impactor velocity on the initial velocity is presented (Fig. 5). Negative residual velocities indicate that the impactor did not penetrate the target and was repulsed from it. For the both materials residual impactor velocity depends linearly on the initial impactor velocity when target is penetrated. In general, the ZrO2(Y2O3) ceramics demonstrated much better ballistic performance with a much

higher limit velocity (around 380 m/s) comparing to around 80 m/s for the Al2O3 target. For all the computations in this section 1 μs incubation time was used.

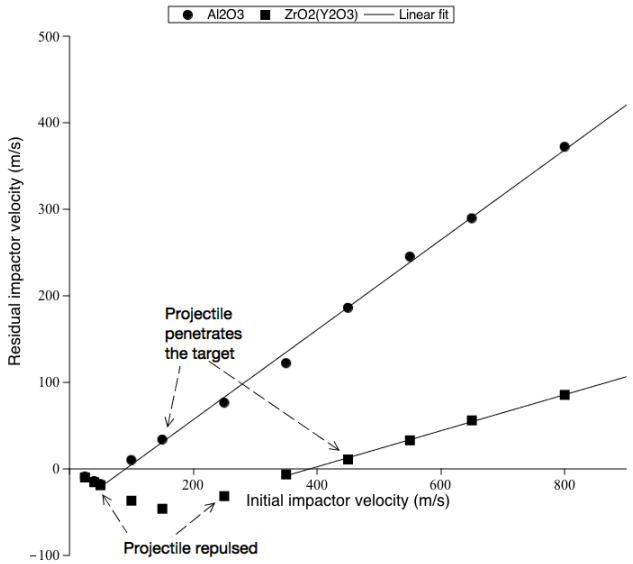

Fig. 5. Residual impactor velocity versus initial impactor velocity

Dynamic fragmentation. Number of fragments. Figure 6 in this section presents dependence of the total number of fragments on the impactor velocity. Higher impactor velocities result in a more extensive target fragmentation and higher total number of fragments. This result naturally correlates with the fracture surface are – impactor velocity dependence (Fig. 4): here number of fragments remains almost constant for the 800 m/s impactor velocity comparing to the value obtained for the 700 m/s velocity.

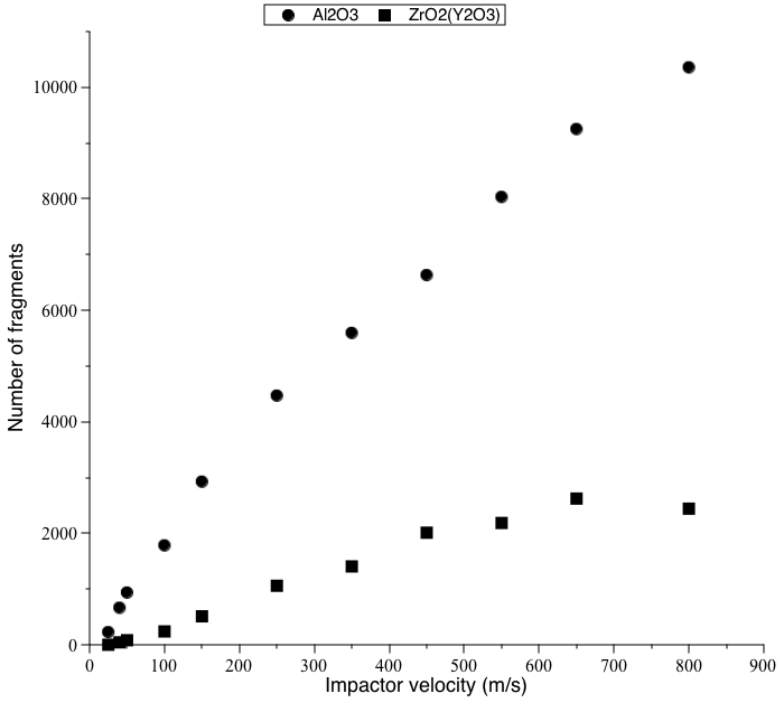

Fig. 6. Number of fragments versus impactor velocity

Dynamic fragmentation. Fragment size distribution. In this section distributions of the fragments are studied. Cumulative size fraction of fragments of all the fragment sizes is

presented using logarithmic scale axes. Size of a fragment is measured as the number of elements it consists of. Experimental investigations of the dynamic fragmentation process usually reveal power law distribution of the fragments [9]. The power law approximation (a straight line on a logarithmic scale) works reasonably well for the small fragment region of the distribution, while discrepancies can be encountered for the larger fragments. Figure 7 shows fragment size distribution reprinted from work [10], where the above-mentioned trend can be observed.

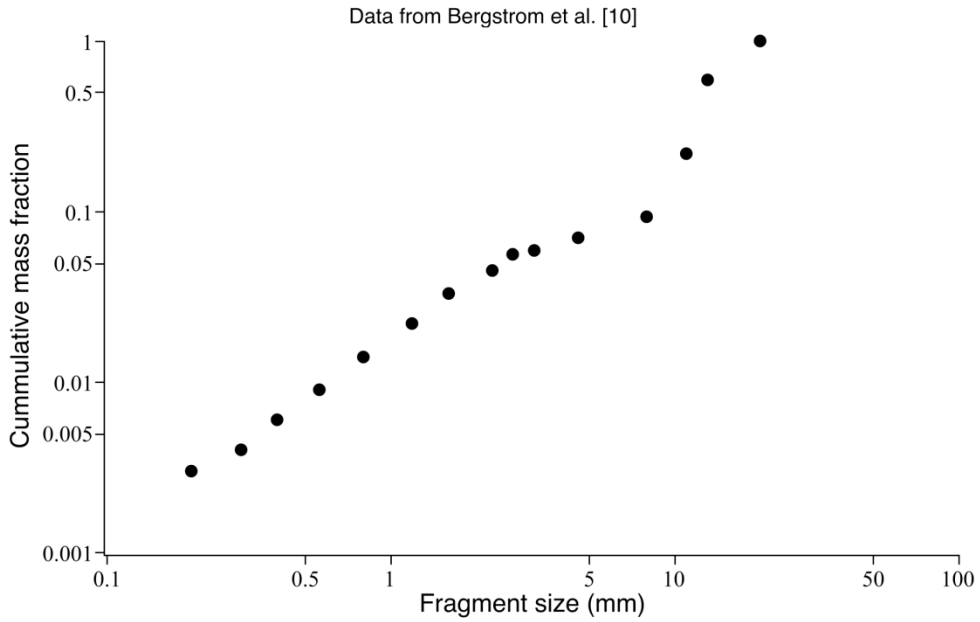

Fig. 7. Experimentally observed fragmentation of glass. The figure is reprinted from work [7]

The obtained numerical results qualitatively resemble experimental data – straight lines are observed for smaller fragments with different behavior for medium and larger fragments. It appears that fragments with particular sizes contribute less comparing to the other fragment sizes. Figure 8 presents typical distributions of the fragments for both materials and 350 m/s impactor velocity. Corresponding fragmentation patterns, showing fragments distinguished by color (excepting for the smallest one-element fragments which are all colored in black) are shown below each graph.

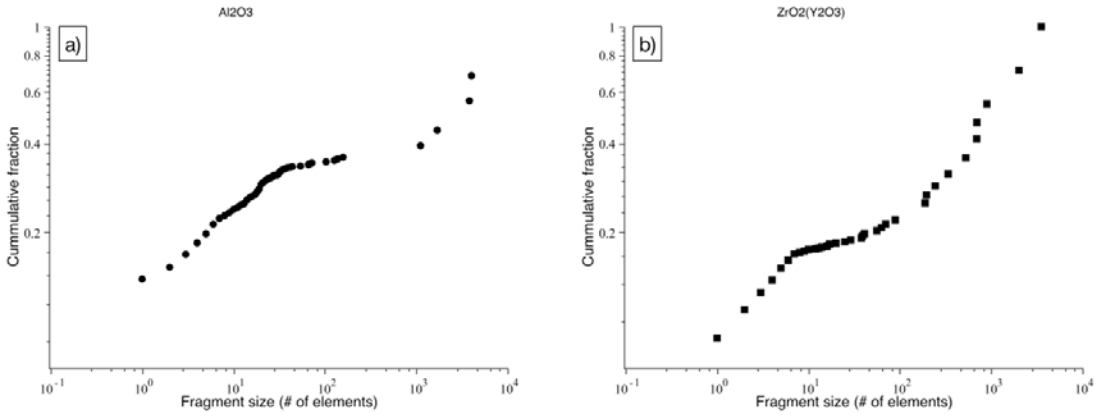

Fig. 8. Cumulative distribution of the fragment sizes and corresponding fragmentation patterns; a) – Al2O3, b) – ZrO2. Left edge of the of the presented fragmentation patterns coincides with the target symmetry axis

5. Conclusions.

In the presented paper performance of two ceramic materials – Al2O3 and ZrO(Y2O3) – under impact loading conditions is compared. The incubation time model is used to predict dynamic fracture. Higher ultimate tensile stress of the ZrO(Y2O3) determined better performance of this materials in terms of penetration resistance. Fragmentation of both materials was also numerically studied: dependence of total number of fragments on the impactor velocity and incubation time value were assessed. In addition to this fragment size distributions were evaluated for various impactor velocities. In all cases the distributions follow the power law (straight line in logarithmic coordinates) for the small fragments, while discrepancies are observed for larger fragments. Such behavior is common for the dynamic fragmentation of brittle materials.

Acknowledgements. *The work was supported by Russian Science Foundation (grant 18-71-00107).*

References

[1] Healey A, Cotton J, Maclachlan S, Smith P, Yeoman J. Understanding the ballistic event: methodology and initial observations. *Journal of Materials Science.* 2017;52(6): 3074-3085.

[2] Petrov YV, Utkin AA. Dependence of the dynamic strength on loading rate. *Soviet Materials Science.* 1989;25(2): 153-156.

[3] Bratov VA, Kazarinov NA, Petrov YV. Numerical implementation of the incubation time fracture criterion. *Journal of Physics: Conference Series.* 2015;653(1): 012049.

[4] Petrov YV. On "quantum" nature of dynamic failure of brittle media. *Dokl. Akad. Nauk SSSR.* 1991;321(1): 66-68.

[5] Evstifeev A, Kazarinov N, Petrov Y, Witek L, Bednarz A. Experimental and theoretical analysis of solid particle erosion of a steel compressor blade based on incubation time concept. *Engineering Failure Analysis.* 2018;87: 15-21.

[6] Masaki T. Mechanical Properties of Toughened ZrO_2-Y_2O_3 Ceramics. *Journal of American Mechanical Society.* 1986;69(8): 638-640.

[7] Winnbust AJA, Keiser K, Burggraaf AJ. Mechanical Properties and Fracture Behaviour of ZrO_2-Y_2O_3 Ceramics. *Journal of Materials Science.* 1983;18(7): 1958-1966.

[8] Jiusti J, Kammer EH, Neckel L, Lóh NJ, Trindade W, Silva AO, Montedo ORK, De Noni Jr. A. Ballistic performance of Al_2O_3 mosaic armors with gap-filling materials. *Ceramics International.* 2017;43(2): 2697-2704.

[9] Grady DE. Fragment size distributions from the dynamic fragmentation of brittle solids. *International Journal of Impact Engineering.* 2018;35(12): 1557-1562.

[10] Bergstrom HC, Sollenberger CL, Mitchel W. Energy aspects of single particle crushing. *Trans AIME.* 1961;220: 367-372.